POLITECNICO DI TORINO
Repository ISTITUZIONALE

Plasticization of dialcohol cellulose and effect on the thermomechanical properties

Original
Plasticization of dialcohol cellulose and effect on the thermomechanical properties / Pellegrino, E., Jonasson, K., Fina, A., Lo Re, G.. - In: POLYMER DEGRADATION AND STABILITY. - ISSN 0141-3910. - 235:(2025). [10.1016/j.polymdegradstab.2025.111259]

Availability:
This version is available at: 11583/3001259 since: 2025-06-25T15:15:33Z

Publisher:
Elsevier

Published
DOI:10.1016/j.polymdegradstab.2025.111259

Terms of use:

This article is made available under terms and conditions as specified in the corresponding bibliographic description in the repository

Publisher copyright

(Article begins on next page)

21 November 2026

Polymer Degradation and Stability 235 (2025) 111259

Contents lists available at ScienceDirect

Polymer Degradation and Stability

journal homepage: www.journals.elsevier.com/polymer-degradation-and-stability

Plasticization of dialcohol cellulose and effect on the thermomechanical properties

Enrica Pellegrino [a,b], Katarina Jonasson [a,c,d], Alberto Fina [b], Giada Lo Re [a,*]

[a] Chalmers University of Technology, Department of Industrial and Materials Science, SE-41296, Gothenburg, Sweden
[b] Politecnico di Torino, Department of Applied Science and Technology, 15121, Alessandria, Italy
[c] FibRe, Chalmers University of Technology, Department of Applied Chemical Engineering, SE-41296, Gothenburg, Sweden
[d] Tetra Pak Packaging Solutions AB, SE-22186, Lund, Sweden

ARTICLE INFO

Keywords:
Cellulose
Melt processing
Plasticization
Mechanical recycling
Thermal stability

ABSTRACT

Cellulosic materials are considered good alternatives to conventional plastics in packaging applications, as they are renewable, bio-based and biodegradable, having good mechanical properties at relatively low densities. However, when considering production methods, cellulose has limitations. The possibility of exploiting the production methods of conventional plastics, such as melt processing, is precluded because cellulose decomposes before reaching melting. Lowering the glass transition, partial modification of cellulose pulp to dialcohol cellulose (DAC) fibres enabled a melt processability window between the glass transition and decomposition temperatures. Water was successfully used as an aid for DAC melt processing, but the final material properties are strongly influenced by the residual moisture content, which varies depending on the environmental conditions (temperature and relative humidity). This work aims to explore the addition of glycerol, a less volatile green plasticizer, to control the processability and physical properties of DAC-based materials. Materials containing different moisture and glycerol contents were melt compounded and the effect on the melt processability was evaluated by the in-line melt viscosity during the process. The effect of different initial moisture and glycerol contents on thermal decomposition, thermal transitions, thermomechanical and mechanical properties and surface morphology has been investigated. The addition of glycerol allows for improved melt processability, decreased elasticity and enhanced deformability up to a maximum glycerol content. An excess of glycerol leads instead to a neat fall in mechanical properties and thermal stability. The possibility of post-industrial mechanical recycling was also demonstrated and the effect on the thermal decomposition and mechanical properties assessed.

1. Introduction

By 2017, the total global production of plastic had reached 8.3 billion metric tons, with projections indicating a potential increase to 34 billion metric tons by 2050 [1]. The highest demand for disposable food packaging products has been identified as a significant contributor to this growth [2]. The utilisation of fossil-based plastics is giving rise to significant environmental concerns, primarily due to the inadequacy of current recycling methods and the long degradation life of these materials [3]. The development of biodegradable plastics derived from renewable resources, owning favourable mechanical properties, high versatility, low-energy and low-cost production methods is of interest as an alternative to traditional plastics [4]. Of the total global plastic production, just a small part accounts for bioplastic production (~ 1 wt. %), which, however, is undergoing a period of growth; it is anticipated that the capacity for bioplastic production will increase significantly, from approximately 2.18 million tonnes in 2023 to an estimated 7.43 million tonnes by 2028 [5].

Cellulose, the world's most abundant biopolymer, offers a promising sustainable alternative to traditional plastic materials, helping to address the environmental issues linked to single-use plastics [6]. The molecular structure of cellulose is composed of glucose units connected by β−1,4 glycosidic bonds [7]. In addition to being biodegradable and renewable, cellulose has a complex hierarchical structure that extends from the nanoscale to the macroscale, offering excellent mechanical properties while maintaining a relatively low density [4]. The

* Corresponding authors.
E-mail address: giadal@chalmers.se (G. Lo Re).

https://doi.org/10.1016/j.polymdegradstab.2025.111259
Received 31 October 2024; Received in revised form 27 January 2025; Accepted 7 February 2025
Available online 8 February 2025
0141-3910/© 2025 The Authors. Published by Elsevier Ltd. This is an open access article under the CC BY license (http://creativecommons.org/licenses/by/4.0/).

development of a hierarchical structure is primarily influenced by the strong intermolecular forces between cellulose chains [8,9]. However, these forces hinder the use of conventional plastic production methods, *e.g.* melt processing, as cellulose-based materials start to decompose well before reaching a molten state [4,10]. The melt processing of cellulose represents a solvent-free, cost-effective, and energy-efficient production method that could enable the fabrication of complex 3D-shaped packaging materials with a wide range of potential applications [11]. Cellulose melt processing could be obtained by developing solutions that allow the loosening of the intermolecular interactions. Chemical modification of hydroxyl groups would allow for the partial disruption of the mutual interactions between cellulose chains, enabling the material to have a thermoplastic behaviour (appearance of a glass transition temperature T_g before decomposition) [4]. The melt processing of the most commonly used cellulose derivatives (chemical modification by esterification and etherification [12]) is highly dependent on the degree of substitution and remains challenging because of a narrow gap between glass transition and decomposition temperatures [13,14]. High degrees of substitution, resulting in greatly reduced crystallinity, and large quantities of plasticizers are required to allow melt processability. These features reduce the viscosity during the processing and result in a lowering of the final mechanical properties.

Cellulose chemical modification to dialcohol cellulose (DAC) fibres has shown some advantages compared to the commonly used cellulose derivatives. The modification is obtained by an oxidation reaction with sodium periodate, which can selectively break the C_2–C_3 bonds in the glucopyranose backbone of cellulose, and by the following reduction with sodium borohydride which converts the so formed aldehydes into hydroxyl groups (Fig. 1a) [15]. The opening of the glucopyranose ring in cellulose structure allows for improved cellulose chain mobility [16]. Considering the degree of modification (DOM) as the percentage of open C_2–C_3 bonds, a decrease in cellulose crystallinity is observed by increasing the DOM [17]. The modification from crystalline cellulose to amorphous DAC is hypothesised to progress gradually from the fibres surface towards their inner core, creating a core-shell structure (Fig. 1a) [18] capable of retaining some of the crystallinity of the native cellulose, and thus the mechanical properties. It has also been demonstrated that increasing the DOM enables a reduction in the glass transition temperature (T_g) assessed by differential scanning calorimetry (DSC) and dynamic-mechanical analysis (DMA), implying a widening of the processing window [16]. Despite the establishment of a T_g, the addition of a plasticizer is still necessary to favour the DAC melt processability. The addition of a plasticizer would serve as a spacer between the DAC chains, reducing their mutual interactions and resulting in a reduction in material's T_g. This would improve the melt processability but also the deformability, reducing rigidity [19]. Water has been successfully used as a temporary plasticizer, as an aid to improve DAC melt processability [11,20–22]. Water has the advantages of being a green, non-toxic, abundant and cheap plasticizer; however, its evaporation during processing is energy demanding and its content varies during storage, so that material's properties vary widely according to the surrounding conditions, *e.g.*, humidity and temperature [23].

A minimal retention of 30 wt.% of moisture is required for a stable secondary shaping of DAC [11]. Therefore, this work aims to investigate

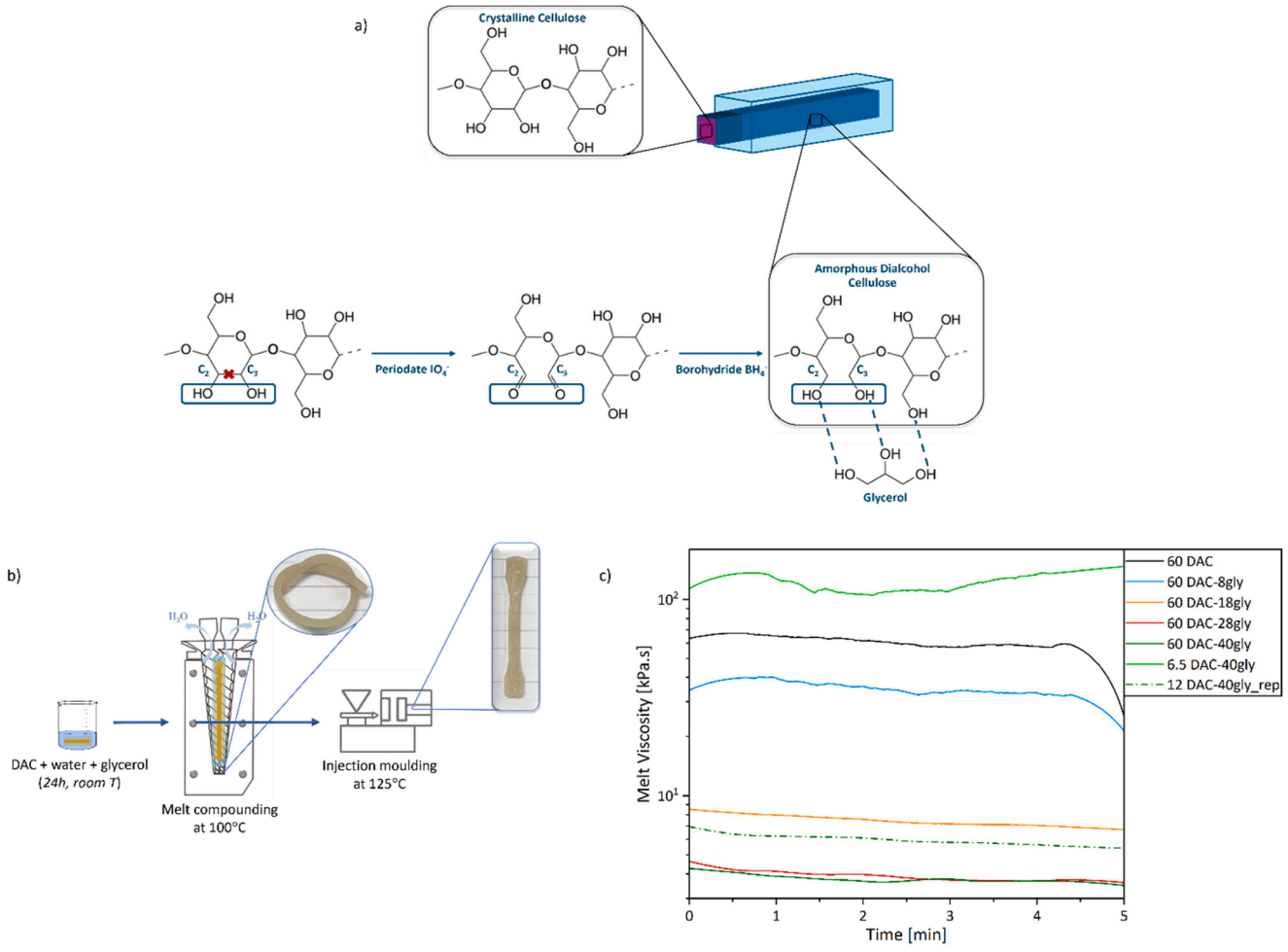


Fig. 1. Chemical modification of cellulose fibres into DAC fibres and their interactions with glycerol molecules (a). Schematic melt processing design (b) and in-line melt viscosity during melt compounding (c) of the materials melt compounded with different moisture (60, 12 and 6.5 phr) and glycerol (0,8,18,28, 40 phr) contents.

the possibility of partially substituting water with a less volatile green plasticizer to enable a stable secondary melt processing, *e.g.* injection moulding, and to reduce the material's properties dependence on external environmental conditions. Glycerol is one of the most widely used plasticisers for cellulose and its derivatives [24], but also for other polysaccharides like starch [24–29] and chitosan [30]. Glycerol has many advantages as it is biodegradable, heat resistant and non-toxic [31]. Its chemical structure, composed of three hydroxyl groups, and its small size allow it to interact easily with cellulose chains, reducing their mutual bonds (Fig. 1a). Due to its hygroscopicity, glycerol can also easily interact with water [23,32,33]. Water and glycerol have been used for DAC plasticization during melt compounding and secondary 3D-shaping with injection moulding. The effect of the addition of varying moisture and glycerol contents on different material properties has been investigated. Additionally, the mechanical recycling of the material melt compounded with the highest moisture and glycerol contents has been performed after pellets conditioning (7 days at 23 °C and 50% RH), and the reprocessing effect has been studied on materials properties. The improvement in melt processability has been evaluated with in-line melt viscosity during melt compounding, thermal stability with a thermal gravimetric analysis (TGA), chemical interactions between the components with infrared spectroscopy (ATR-FTIR), thermal transitions with temperature modulated differential scanning calorimetry (MDSC), mechanical properties with tensile test, viscoelastic behaviour with dynamic thermal mechanical analysis (DMTA) and cryo-fractured surface morphology with scanning electron microscopy (SEM).

2. Materials and methods

2.1. Materials

DAC with a 46% DOM, derived from bleached softwood kraft pulp fibres (K48), was kindly supplied by SCA Forest Products (Östrand pulp mill, Timrå, Sweden) in form of sheets (at equilibrium moisture content of 6 wt.%). The chemical modification was obtained following the method reported by Larsson et al. [17,34]. Sodium periodate was used to partially oxidize cellulose into dialdehyde cellulose, breaking the C_2—C_3 bond in the glucopyranose ring. The oxidation was followed by a reduction using sodium borohydride to reduce the aldehyde groups into alcohol groups. The degree of modification (DOM) was assessed by the aldehyde content after periodate oxidation applying a well-established protocol based on a reaction with hydroxylamine hydrochloride [35]. Deionized water and glycerol (Sigma Aldrich), used as received, were mixed and added to the sheets.

2.2. Evaluation of the moisture content

The materials moisture content, evaluated after each processing step, was assessed by drying samples for 48 h in an oven at 70 °C. Weight loss was monitored every 6 h and already after 36 h no weight changes were recorded supporting our choice of drying the material for 48 h to determine the water content at equilibrium. Measurements were performed in triplicates and reported as mean values.

2.3. Melt processing of DAC + water + glycerol systems: compounding and injection moulding

Different materials were obtained by changing both moisture and glycerol contents. For some materials, the moisture content was fixed (60 parts per 100 parts of dry DAC) while the glycerol content increased (0, 8, 18, 28 and 40 parts per 100 parts of dry DAC). The mixtures were prepared by dissolving the selected amount of glycerol in the chosen amount of water; the solutions were then poured on the DAC fibre sheets. The mixtures were stored in sealed bottles for 24 h to allow the fibres to absorb water, or water/glycerol solutions, or glycerol alone while limiting water evaporation before the melt compounding. The melt compounding was performed in a micro-compounder (Xplore, Maastricht, The Netherlands). The following processing conditions were used: temperature of the micro-compounder (100 °C), residential time (15 + 5 min), screw speed (15 + 60 rpm), and amount of solid material to compound (glycerol + DAC = 20 g). After the extrusion of the material containing the highest glycerol content (40 parts per 100 parts of dry DAC), the pellets were conditioned for 7 days at 23 °C and 50 % relative humidity (RH). The pellets weight was monitored every 12 h and already after 4 days no further weight change was observed, indicating the achievement of the equilibrium conditions. To ensure the achievement of the equilibrium state, 7 days have been selected as the conditioning time. After the conditioning, the pellets were reprocessed in the same conditions selected for the other materials, starting from the equilibrium moisture content for that sample (12 parts per 100 parts of dry DAC at 23 °C and 50 % relative humidity (RH)). For one last material, the highest selected glycerol content (40 parts per 100 parts of dry DAC) was directly added to the DAC sheets without the addition of external water (DAC equilibrium moisture content of 6.5 parts per 100 parts of dry DAC at 23 °C and 50 % relative humidity (RH)).

Table 1 reports the different glycerol contents before compouding, the moisture content before compounding and the water loss during compounding. In the nomenclature, the first number is associated with the moisture content before compounding (expressed as parts per hundred parts of resin, phr) while the second to the glycerol content before compounding (expressed as parts per hundred parts of resin, phr).

The injection moulding was performed in a micro-injection moulding (Xplore, Maastricht, The Netherlands), right after the compounding to maintain the same moisture content possessed by the extruded material. The following parameters were used for the injection moulding: temperature of the injector (125 °C), temperature of the mould (30 °C) and pressure imposed on the material (7 bar for 25 s). Rectangular shaped specimens were produced for dynamic thermal mechanical analyses (25 × 5 × 1 mm^3) and dumbbell-shaped specimens for tensile tests (with a gauge length of 25 mm and a thickness of around 2 mm, according to the standard ASTM D638−14).Table 2 reports the moisture content before and after the injection and the final moisture and glycerol content after conditioning of the materials (after 7 days at 23 °C and 50 RH%) (expressed as parts per hundred parts of resin, phr).

2.4. In-line melt viscosity

During the compounding, the micro-compounder registered the torque imposed on the co-rotating screws, and from these values, the equipment software calculated the melt viscosity according to Eq. (1).

$$\eta = \frac{\tau}{\dot{\gamma}} \tag{1}$$

Table 1
Glycerol content before compounding, moisture content before compounding and water loss during compounding. In the acronyms, the first number is associated with the moisture content before compounding (phr) and the second to the glycerol content before compounding(phr).

Material	Glycerol content [phr]	Moisture content before compounding [phr]	Water loss compounding [g]
60 DAC	/	60 ± 3	4.8 ± 2.9
60 DAC-8gly	8 ± 1	60 ± 3	3.5 ± 2.6
60 DAC-18gly	18 ± 1	60 ± 3	2.5 ± 2.5
60 DAC-28gly	28 ± 1	60 ± 3	2.3 ± 2.3
60 DAC-40gly	40 ± 1	60 ± 3	2.2 ± 2.2
6.5 DAC-40gly	40 ± 1	6.5 ± 1	/
12 DAC-40gly_rep	40 ± 1	12 ± 1	/

Table 2
Variation of the moisture content before and after the injection, moisture content and glycerol content after the conditioning (* 7 days at 23 °C and 50% RH) (expressed in phr).

Material	Moisture content before injection [phr]	Moisture content after injection [phr]	Moisture content* [phr]	Glycerol content* [phr]
60 DAC	48 ± 3	45 ± 3	6.5 ± 1	/
60 DAC-8gly	47 ± 3	45 ± 3	7 ± 1	8 ± 1
60 DAC-18gly	50 ± 3	48 ± 3	9 ± 1	18 ± 1
60 DAC-28gly	50 ± 3	50 ± 3	11 ± 1	28 ± 1
60 DAC-40gly	48 ± 3	46 ± 3	12 ± 1	40 ± 1
6.5 DAC-40gly	6.5 ± 1	6.5 ± 1	12 ± 1	40 ± 1
12 DAC-40gly_rep	12 ± 1	12 ± 1	12 ± 1	40 ± 1

Where $\dot{\gamma}$ is the shear rate (recorded by the equipment) and τ is the shear stress (proportional to the torque).

2.5. Thermal gravimetric analysis (TGA)

A thermal gravimetric analysis (TGA) was performed using a TGA/differential scanning calorimetry (DSC) 3 + Star system (Mettler Toledo, Greifensee, Switzerland). 4–5 mg of the materials were first heated for 60 min at 105 °C to let most of the water evaporate and then a temperature ramp from 105 °C to 500 °C was performed with a heating rate of 10 °C/min. Measurements were performed under dry N_2 gas Measurements were performed in duplicates. The materials, before being tested, were conditioned for 7 days at 23 °C and 50 RH%.

2.6. Attenuated total reflection-Fourier transformed infrared (ATR-FTIR)

ATR-FTIR spectra of the samples were acquired with a Frontier FT-IR Spectrometer in ATR mode (Perkin Elmer, Shelton, Connecticut). 32 scans were performed from 4000 to 400 cm^{-1} with a resolution of 4 cm^{-1}. Measurements were performed in duplicates. The materials, before being tested, were conditioned for 7 days at 23 °C and 50 RH%.

2.7. Modulated Differential Scanning Calorimetry (MDSC)

Modulated Differential Scanning Calorimetry (MDSC) tests were performed with a Q20 DSC (TA Instruments, USA) on samples of *ca.* 9 mg in closed aluminium pans with perforated lids. By overlapping temperature periodic oscillations on a constant heating/cooling rate, this approach enables the separation of the total heat flow into the reversing heat flow, associated with the changing heating rate (heat capacity related events) and the non-reversing heat flow, associated with the time and temperature dependent component. The average heating rate was set at 2 °C/min, the temperature modulation period at 80 s, the temperature modulation amplitude at ± 0.4 °C in a temperature range between –20 and 110 °C. Measurements were performed under dry N_2 gas. Measurements were performed in duplicates. The second heating was considered to study the thermal transitions. The materials, before being tested, were conditioned for 7 days at 23 °C and 50 RH%.

2.8. Dynamic mechanical thermal analysis (DMTA)

DMTA was performed with a Q800 DMA (TA Instruments, New Castle, Delaware) operating in the tensile mode. The oscillation frequency and amplitude were 1 Hz and 10 μm, respectively, and temperature scans were performed at a rate of 3 °C/min in the temperature range of −20–150 °C. Measurements were performed in triplicates. The materials, before being tested, were conditioned for 7 days at 23 °C and 50 RH%.

2.9. Tensile test

Dumbbell shaped specimens were tested for each material, with a Zwick/Z2.5 tensile tester (Zwick, Germany) equipped with a load cell of 2 kN and at a strain rate of 10%. The Zwick testXpert software was used to record force and crosshead travel data. Measurements were performed in triplicates. The materials, before being tested, were conditioned for 7 days at 23 °C and 50 RH%.

2.10. Scanning electron microscopy

The cryo-fractured surface's morphology of the different materials was investigated using a Scanning Electron Microscope ZEISS EVO 15 model (ZEISS, Oberkochen, Germany) with an imaging beam voltage of 20eV. Samples were gold sputtered before imaging.

3. Results and discussion

3.1. Melt processability

Under the rational of favorable hydrogen bonding interactions, neat and glycerol plasticized DAC (Fig. 1a) materials were melt processed by using water as a processing aid [11]. Melt processing, *i.e.* melt compounding and injection moulding, was successfully carried out according to the chosen process design (Fig. 1b) on all selected compositions (Table 1). The visual aspect of both the extruded and injection moulded materials is not affected by the composition, therefore representative images after compounding and after injection moulding of 60 DAC-40gly are reported. A decrease in-line melt viscosity during the residential time in the extruder (5 min) was registered by increasing the glycerol content on the DAC moisturized at 60 phr of water (Fig. 1c), resulting in improved melt processability.

However, the melt viscosity does not progressively decrease increasing the glycerol content; above a certain glycerol addition (contents higher than 18 phr) the melt viscosity does not change significantly. This could be ascribed to the creation of continuous glycerol layer on DAC fibre surfaces which hinders their mutual interactions. Therefore, adding an excess of glycerol is not beneficial for improving the melt processability.

It is worth focusing on the results observed for the materials melt compounded with the same glycerol content (40 phr). The addition of water leads to a significant reduction in melt viscosity during compounding for 60 DAC-40gly compared to 6.5 DAC-40gly. In addition, the presence of water during the 60 DAC-40gly compounding would probably allow a uniform distribution between DAC and glycerol, so that the conditioned pellets can be reprocessed (12 DAC-40gly_rep) with significantly lower melt viscosities compared to 6.5 DAC-40gly. Due to the lower initial moisture content, 12 DAC-40gly_rep shows higher viscosities during compounding compared to 60 DAC-40gly, but this increase is lower compared to the viscosity values of 6.5 DAC-40gly.

Higher melt viscosities are associated with higher shear forces applied to the DAC fibres during compounding, which could result in different material properties after extrusion, evaluated in more detail in Section 3.5.2.

The water loss during compounding (Table 1) is found to decrease as the glycerol content is increased. This reduction may be attributed to the interactions between water molecules and the hygroscopic glycerol [23,32,33], which prevent water evaporation. These considerations may

also be linked to the slight increase in equilibrium moisture content observed after conditioning, which appears to be proportional to the increase in glycerol content [30,36,37]. It is worth to note that starting from the equilibrium moisture content prior compounding (6.5 DAC-40gly and 12 DAC-40gly) the water is kept during the melt compounding at 100 °C due to the short residence time (5 min) and the limited exposure to the environment in the microcompounder.

3.2. Thermal stability assessed by TGA

The materials thermal stability was evaluated using a thermal gravimetric analysis (TGA) (Fig. 2). An initial isotherm step at 105 °C was conducted to limit the contribution of the evaporating water during the temperature ramp, in accordance with previous research which has reported a first weight drop at lower temperatures (below 120 °C) associated with the evaporation of bounded water [33,38–41].

The materials not containing glycerol (DAC and 60 DAC) show two main decomposition steps (Fig. 2a and b). From the derivative of the weight percentage as a function of temperature (Fig. 2c and d), two peaks are observed: one peak at ~276 °C can be ascribed to the decomposition of the amorphous dialcohol cellulose regions, while the one at ~350 °C, to the decomposition of the crystalline cellulose regions [11]. The material melt compounded using only water as a temporary plasticizer shows a slight decrease in the onset temperature (Table 3) and in the decomposition temperatures (Table 3) of the amorphous and crystalline regions compared to the native DAC.

The materials melt compounded with a fixed moisture (60 phr) but different glycerol (0,8,18,28, 40 phr) contents show three main decomposition steps, the first step being related to the glycerol volatilization [33,38,39,41]. From the weight loss curve (Fig. 2a), it is possible to appreciate the complete thermal volatilization of pure glycerol after 224 °C; this is also reflected in a decrease in the onset temperature for the material containing glycerol. The onset temperatures decrease with the increase in the glycerol content, but not in a proportional way. Comparing the experimental and calculated onset temperatures and weight at 224 °C (pure glycerol volatilization temperature)(Table 3), it is observed how the experimental values are higher compared to the calculated ones. These results point at an interaction between DAC fibres and glycerol molecules, which delays the glycerol thermal volatilization. Glycerol is dispersed in the DAC matrix, which affects its diffusion rate outside the material. 60 DAC-8gly shows the highest onset temperature, which is ≈ 14 °C and ≈ 11 °C lower compared to native DAC and 60 DAC, and ≈ 38 °C higher compared to the calculated onset temperature; the difference between the experimental and calculated onset temperatures decreases by increasing the glycerol content. At 224 °C, the weight loss of 60 DAC-8gly is only 33% of the calculated one, and this percentage increases together with the glycerol content. These results suggest a stronger interaction between DAC fibres and glycerol

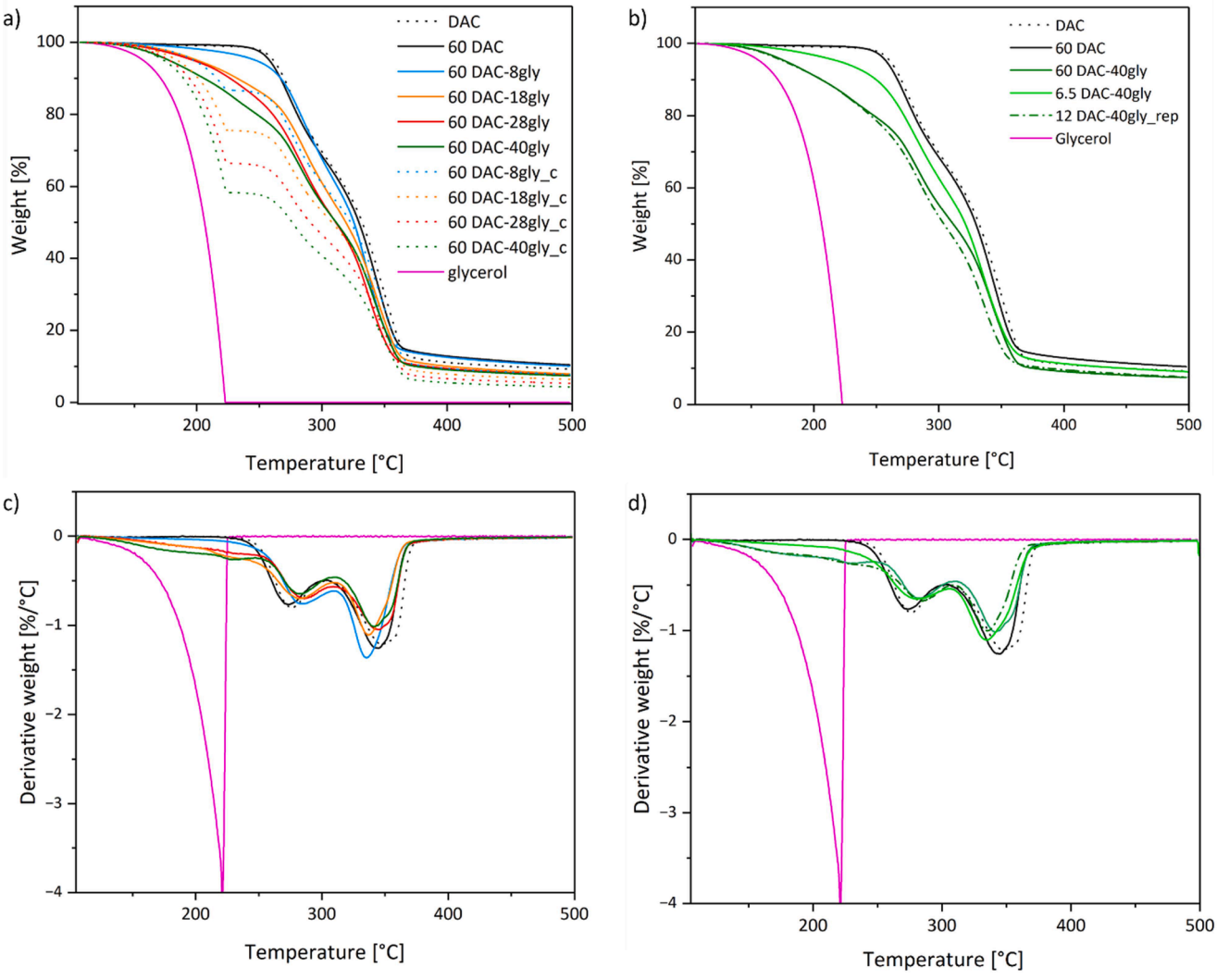


Fig. 2. Weight percentage as function of temperature (a and b), and its derivative (c and d) performed on the native DAC, glycerol and the materials melt compounded with different moisture (60, 12 and 6.5 phr) and different glycerol (0,8,18,28, 40 phr) contents.

Table 3
Experimental and calculated onset temperatures (considered as the temperature at which 5% weight is lost), experimental and calculated weight at 224 °C and residues at 500 °C, decomposition temperatures T_{d1} and T_{d2} (considered as the temperatures in which a peak in the DTG is observed) of the native DAC, glycerol and the materials melt compounded with different moisture (60, 12 and 6.5 phr) and glycerol (0,8,18,28, 40 phr) contents.

Material	Experimental $T_{5\%}$ [°C]	Calculated $T_{5\%}$ [°C]	Experimental weight$_{@\ 224\ °C}$ [%]	Calculated weight$_{@\ 224\ °C}$ [%]	Experimental residue$_{@\ 500\ °C}$ [%]	Calculated residue$_{@\ 500\ °C}$ [%]	T_{d1} [°C]	T_{d2} [°C]
DAC	261	/	/	/	9	/	276	350
60 DAC	258	/	/	/	10	/	274	345
60 DAC-8gly	247	209	97	91	10	8	284	335
−60 DAC-18gly	201	193	92	84	8	7	286	345
60 DAC-28gly	197	186	91	77	8	7	281	337
60 DAC-40gly	178	180	86	70	7	6	280	341
12 DAC-40gly_rep	177	180	86	70	8	6	284	335
6.5 DAC-40gly	220	180	95	70	9	6	280	334
Glycerol	157	/	0	/	0	/	221	/

molecules in 60 DAC-8gly, that effectively slow down the glycerol diffusion. At the highest temperature of the ramp (500 °C) (Table 3), the DAC without glycerol presents the highest residue content, while the systems containing glycerol show a residue value that decreases together with increased glycerol content [38]. Those values are slightly higher compared to the calculated values. From the derivative of the weight percentage as a function of temperature (Fig. 2c), while 60 DAC-8gly presents only two peaks, 60 DAC-18gly and 60 DAC-28gly show a shoulder centred at 228 °C and 60 DAC-40gly a peak at 228 °C, due to the presence of glycerol. A glycerol excess can lead some DAC chain to approach each other, forming hydrogen bonds and showing incomplete plasticization, which results in the aggregation of some glycerol molecules of which a volatilization peak is observed [38,39]. An increase in the decomposition temperatures assigned to the glycerol-plasticized amorphous regions (T_{d1}) (from 274 for 60 DAC up to a maximum of 286 °C for 60 DAC-18gly) is observed, due to the establishment of intermolecular interactions between amorphous DAC and glycerol which improved the materials thermal stability [38,42].

Comparing the materials melt compounded with the same glycerol (40 phr) and different moisture (0,8,18,28, 40 phr) contents, some conclusions can be drawn. The reprocessed material (12 DAC-40gly_rep) exhibits a weight loss and first derivative curves similar to that observed for 60 DAC-40gly (Fig. 2b and d). This indicates that the material's reprocessing does not have a great impact on thermal stability. The sample that was compounded without the addition of water (6.5 DAC-40gly) exhibits significantly enhanced thermal stability compared to 60 DAC-40gly (the 6.5 DAC-40gly onset temperature is ≈ 42 °C higher compared to the one of 60 DAC-40gly) (Fig 2b and d). The reason for this may be that the glycerol, which was added during compounding, was not effectively incorporated into the extruded material, resulting in a lower plasticizer content than the expected value. Consequently, the material contained less plasticiser, which led to a higher experimental onset temperature and weight at 224 °C (pure glycerol volatilization temperature) and at 500 °C than those calculated and observed for 60 DAC-40gly (Table 3).

3.3. *Attenuated total reflection-Fourier transformed infrared spectroscopy*

ATR-FTIR analyses (Fig. 3) were performed after the materials conditioning, so that the final moisture contents to be considered are the ones reported in Table 2.

DAC spectrum shows the peaks characteristic of cellulose for O—H stretching, C—H stretching, absorbed H_2O, CH_2 bending in CH_2OH, CH_2 wagging, C—O-C stretching, C—O stretching and glucose ring stretching at 3315, 2920–2886, 1647, 1420, 1315, 1106, 1010 and 897 cm^{-1} respectively [43–45]. The broad peaks observed at 3315 cm^{-1} in DAC and at 3274 cm^{-1} in glycerol spectra are associated to the O—H stretching, which could be related to the intensity of the established inter- and intramolecular hydrogen bonds [46] and with the presence of strongly bounded water molecules. Absorption band of free hydroxyl groups cannot be clearly distinguished at 3600 cm^{-1}, suggesting that the hydroxyl groups are generally associated with inter- and intramolecular

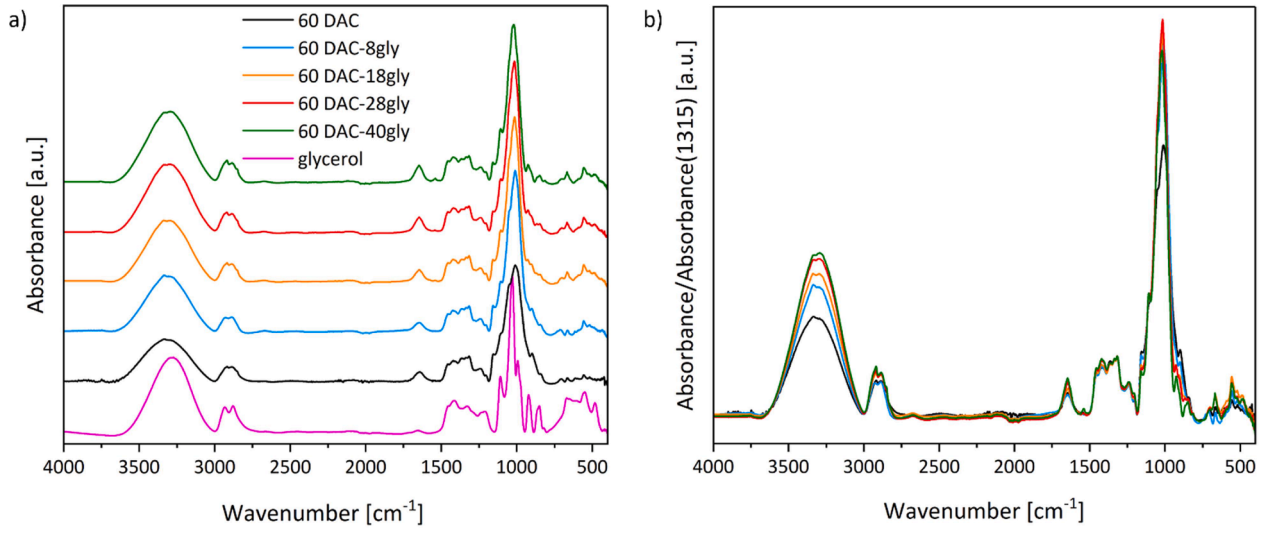


Fig. 3. ATR-FTIR spectra of the materials melt compounded with fixed moisture content (60 phr) and different glycerol contents (0, 8, 18, 28, 40 phr) and of glycerol. The spectra are reported in absorbance, and the values are normalized to the 1315 cm^{-1} peak intensity. This peak is ascribed to the CH_2 wagging and selected as a signal unaffected by the presence of glycerol in the system. Fig. 3a allows for a comparison of the peak's positions, while Fig. 3b allows for a comparison of the peak's intensities.

hydrogen bonding [46,47]. In the DAC materials containing different glycerol contents, a shift of the peak at 3315 cm^{-1} is not observed (Fig. 3a), meaning that the hydrogen bonds strength does not vary. However, an increase in the signal intensity can be appreciated by increasing the glycerol content (Fig. 3b). This could be connected both to an increase in hydroxyl groups number, due to the addition of glycerol, but also to the rise in the moisture absorption by increasing the glycerol content (also observed in the moisture content values after conditioning) [33,38,48]. Two peaks at 2920 and 2886 cm^{-1} in the DAC spectrum are associated with the C—H stretching; the same peaks are observed at 2933 and 2879 cm^{-1} in the glycerol spectrum. In the DAC materials containing glycerol, the second peak does not shift. In contrast, the first peak presents a shoulder at a higher wavenumber, in agreement with the highest wavenumber observed for this peak in the glycerol spectrum (Fig. 3a). This confirms the presence of glycerol in the compositions. The peak at 1647 cm^{-1} is associated with the vibration of water molecules absorbed in cellulose. In the DAC materials containing glycerol, a shift is not observed (Fig. 3a), but an increase in the peak intensity by increasing the glycerol content could be ascribed to more bounded water molecules (Fig. 3b).

In the DAC materials containing glycerol, the peaks at 1106 cm^{-1}, associated with the C—O-C stretching, don't show any shift. The peaks observed at 1010 cm^{-1} in DAC and at 1033 cm^{-1} in glycerol, associated to the C—O stretching, shifts to higher wavenumber due to the presence of increasing glycerol contents (Fig. 3a). The peak at 897 cm^{-1} in DAC slowly decreases in intensity while the peak at 925 cm^{-1} associated with C—OH stretching in glycerol molecules, appears and increases in intensity increasing the glycerol content. The intensities of the peaks in the range between 1150 and 800 cm^{-1} (Fig. 3b) increases by increasing the glycerol content. This can be associated with the establishment of interactions between the functional groups of cellulose and the -OH groups of glycerol [38].

Spectroscopic analyses confirm DAC-glycerol interactions, indicating the effective plasticization of DAC fibres using glycerol [37], later confirmed by MDSC, DMTA and tensile test. The increase in absorbed water by adding glycerol is also confirmed by the increased intensity of the peak at 1647 cm^{-1} pointing at an increased water sensitivity due to the use of glycerol for the DAC plasticization.

3.4. Thermal transitions assessed by temperature-modulated differential scanning calorimetry

Preliminary tests were performed using a traditional differential scanning calorimetry test (DSC), which made it difficult to detect thermal transitions, *e.g.* glass transition temperatures (T_g). Accordingly, a temperature-modulated DSC was selected. The reverse heat flow (Fig. 4c) shows the subtraction from the total heat flow of the time and temperature dependent components (non-reversing heat flow).

Low intensity signals are observed from the total heat flow curves (Fig. 4a), however, for 60 DAC, 60 DAC-8gly and 60 DAC-28gly, exothermic steps are visible. Similar steps are also seen around the same temperature in the non-reversing heat flow. From the reversing heat flow (Fig. 4c), a step connected to the change in heat capacity around the T_g is clearly observed. The curves illustrated represent the second heating curves, wherein it is assumed that the water present after conditioning has evaporated from the materials (moisture contents after conditioning for 7 days at 23 °C and 50% RH in Table 2). As the glycerol content increases, the step-related to T_g is observed at decreasing temperatures (from 58 °C for 60 DAC to 4 °C for 60 DAC-40gly, Table 4). As demonstrated by ATR-FTIR spectra, glycerol molecules interact with DAC chains, lowering their intermolecular bonds. These interactions and a good glycerol dispersion in the matrix lead to a plasticizing effect which is reflected in the gradual decrease in T_g by adding increasing glycerol contents [49–51].

It is worth noting that in the range of scanned temperatures, only a single transition is visible in the thermograms of the tested materials. Glycerol glass transition occurs at lower temperature compared to the ones used for the test (T_g glycerol ~ −86 °C [52]), therefore, a transition connected to a glycerol phase separation, or a glycerol-rich phase are not detectable in this temperature range [53,54]. In a previous work reported by *Östberg* et al. [55], an endothermic peak is observed at a lower temperature during the first heating ramp when moisture content in

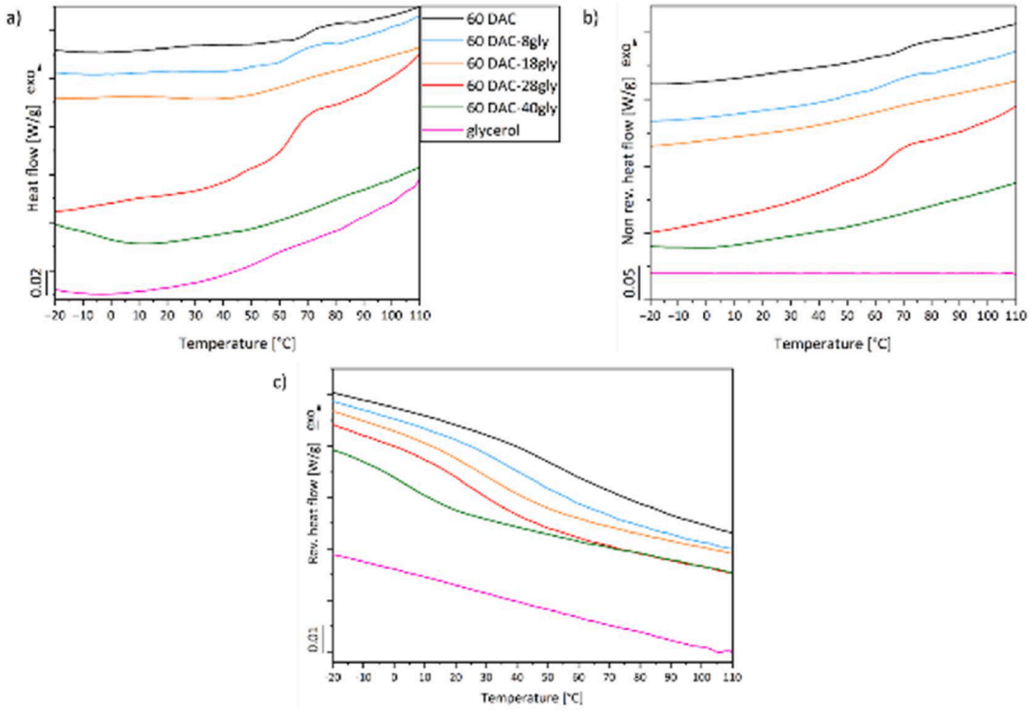


Fig. 4. Total (a), non-reversing (b) and reversing heat flow (c) as a function of temperature obtained by MDSC performed on glycerol and the materials melt compounded with fixed moisture (60 phr) and different glycerol (0,8,18,28, 40 phr) contents.

Table 4
T_g extrapolated from the flexural points of the reversing heat flow by MDSC. Young's modulus, stress at break and elongation at break obtained by tensile test analysis. storage modulus at three different temperatures (−30, 30 and 150 °C) and alpha transition temperatures T_α (~T_g,) obtained evaluating the variation of the storage modulus and of the tanδ in a temperature ramp during DMTA. The tests were performed on the materials melt compounded with different moisture (60, 12 and 6.5 phr) and glycerol (0,8,18,28, 40 phr) contents.

Material	T_g [°C]	Young's Modulus [MPa]	Stress at break [MPa]	Elongation at break [%]	$E_{-20\ °C}$ [MPa]	$E_{30\ °C}$ [MPa]	$E_{150\ °C}$ [MPa]	T_α [°C]
60 DAC	58	487 ± 40	14.8 ± 1.0	43 ± 2	8134 ± 183	2200 ± 52	85 ± 14	35 ± 2
60 DAC-8gly	48	247 ± 23	11.5 ± 0.6	61 ± 7	5310 ± 870	681 ± 160	57 ± 8	22 ± 4
60 DAC-18gly	28	118 ± 8	7.4 ± 0.2	77 ± 2	2966 ± 700	181 ± 41	41 ± 4	6 ± 1
60 DAC-28gly	21	10 ± 2	2.2 ± 0.3	55 ± 4	514 ± 52	35 ± 0,5	18 ± 2	−0,5 ± 0,5
60 DAC-40gly	4	6 ± 3	1.8 ± 0.3	46 ± 6	285 ± 20	27 ± 2	17 ± 1	−6 ± 0,2
12 DAC-40gly_rep	/	2.7 ± 0.2	0.4 ± 0.1	18 ± 1	/	/	/	/
6.5 DAC-40gly	/	1.7 ± 0.6	0.2 ± 0.1	9 ± 3	/	/	/	/

wood materials is increased. This peak must involve some other phenomenon in addition to the glass transition reversing event, such as non-reversing events like enthalpic relaxation [56]. In this study, the exothermic step observed in the non-reversing heat flow (Fig. 4b) can also be ascribed to some time-dependent events observed above the T_g due to the rearrangement of the fibres.

3.5. Thermo-mechanical properties

3.5.1. Viscoelastic behaviour assessed by dynamic mechanical thermal analysis (DMTA)

The viscoelastic behaviour of the plasticized DAC systems has been evaluated through dynamic mechanical thermal analysis (DMTA) (Fig 5a and b).

Adding a plasticizer leads to a decrease in the storage moduli at every temperature (Fig. 5a, Table 4) due to the softening action of glycerol. Lower storage moduli are observed by adding more glycerol to the

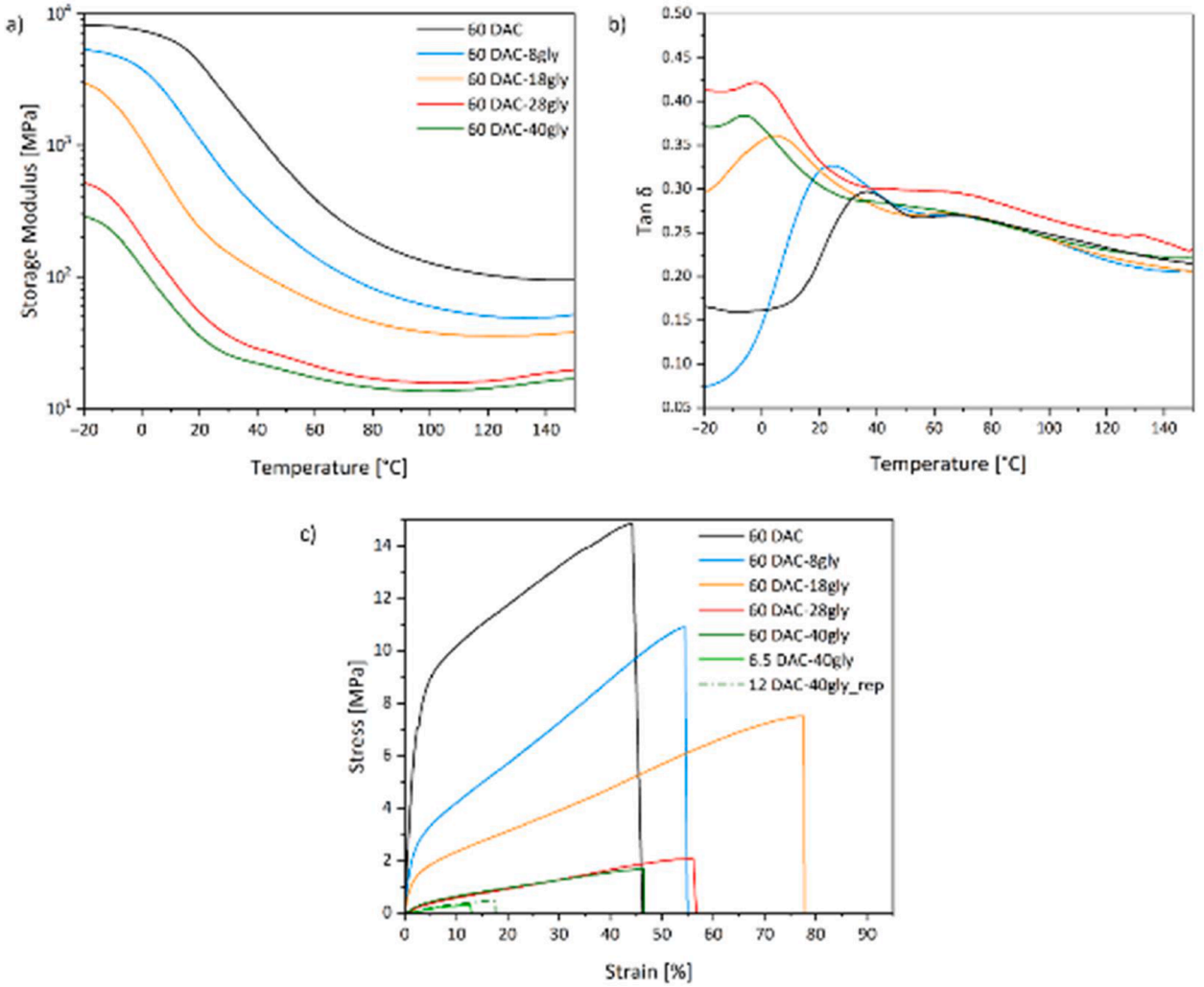


Fig. 5. Representative variation of storage modulus (a) and tanδ (b) with increasing temperature for the materials melt compounded with fixed moisture (60 phr) and different glycerol (0, 8, 18, 28, 40 phr) contents. Representative strain-stress curves (c) for the materials with melt compounded with different moisture (60, 12 and 6.5 phr) and glycerol (0,8,18,28, 40 phr) contents.

system (from 2200 MPa for 60 DAC to 27 MPa for 60 DAC-40gly at 30 °C). The glycerol molecules decrease the intermolecular interactions between DAC chains, helping their mutual sliding, observed by the decrease in the T_α ($\sim T_g$), obtained from the peaks in the tan δ curves (Fig. 5b, Table 4). T_α decreases together with the glycerol content increase [51,57] (from 35 °C for 60 DAC to of −6 °C for 60 DAC-40gly). Also in this case, only one transition is visible in the tested materials, and corresponding a decreased glass transition of the DAC, because the starting temperature at which the test was performed is not low enough to observe a transition connected to glycerol phase separation or to a glycerol-rich phase [53,54]. The different glass-rubber transition temperatures obtained from MDSC and DMTA tests are related to the fact that DMTA tests are performed on samples containing moisture after conditioning (Table 2) and the plasticizing effect of water is observed at lower transition temperatures than the ones observed from MDSC. In addition, the two tests are based on different principles, so the temperatures obtained are not directly comparable. However, the variation of T_α and T_g by inserting different glycerol contents are consistent. Overall, the decrease in the glass-rubber transition temperature represents an increase in the system mobility, which is in agreement with the observed lower in-line melt viscosities during compounding (Fig. 1), corresponding to an improved melt processability of the systems. It is worth noting that the storage moduli show a plateau at high temperatures (above 100 °C). This behaviour can be ascribed to the semi-crystalline structure of the system [57] or to the presence of a network due to multi-hydrogen bond interactions that is only partially affected by the action of increasing temperature. The network is affected by the presence of increasing content of glycerol, as the storage moduli at the plateau decrease by increasing the glycerol content.

3.5.2. Tensile test

All the materials present a strain hardening typical of elastomers up to break due to the alignment of the fibres in the stretching direction. The plasticizing effect of glycerol is observed from the decrease in Young's modulus (from 487 for 60 DAC to 6 MPa for 60 DAC-40gly) and tensile strength (from 14.8 for 60 DAC to 1.8 MPa for 60 DAC-40gly) increasing the glycerol content (Table 4). The tensile behaviour can be also ascribed to the glycerol ability of diminishing the strong intramolecular interactions between the DAC chains, together with the formation of hydrogen bonds between glycerol and DAC chains. Similar trends can be found in other works reporting glycerol effect on the mechanical properties of different materials, in particular cellulose derivatives and starch from different sources [37,46,51,58–64]. The plasticizing effect of glycerol is also observed in an increase in the elongation at break (from 43% to 77%) (Table 4). Glycerol reduces the rigidity and promotes deformability of DAC materials allowing more chain mobility. As reported by Zavareze et al. [65] the elongation of polymeric materials depends on the mobility of their molecular chains. It should be noted that the plasticizing effect is not limited to glycerol, but also applies to the water present in the material at equilibrium. Differently from the results reported in different studies [37,46,58–60], the elongation doesn't increase together with the glycerol content [51,61–64] as for 60 DAC-28gly and 60 DAC-40gly is observed a drop in the deformability (from a maximum of 77% for 60 DAC-18gly to 55% and 46% for 60 DAC-28gly and 60 DAC-40gly). Adding an excess of plasticizer leads the material to became too soft so that no strain hardening stabilizes the material's structure [64]. Another reason is a possible glycerol segregation which allows for faster propagation of cracks [51,64]. This phenomenon occurs when the glycerol concentration overcomes its miscibility in the DAC, causing phase separation [51]. The discussed results demonstrated that glycerol can be successfully used as a plasticizer for DAC, but after a certain amount there is a drop in the materials properties.

It is worth comparing the three materials containing the same glycerol content (60 DAC-40gly, 12 DAC-40gly_rep and 6.5 DAC-40gly). The material melt compounded adding glycerol and water presents the highest mechanical properties (Young's modulus 6 MPa, stress at break 1.8 MPa, elongation at break 46%); these results could be connected to the thermo-mechanical stresses imposed on the materials during compounding. 60 DAC-40gly shows the lowest melt viscosity during compounding (Fig. 1), leading to lower shear stresses imposed on the material. By removing the added water (6.5 DAC-40gly) a strong increase in the in-line melt viscosity (*i.e.* higher shear stresses imposed on the fibres) is observed. As previously reported in another work [11], as DAC is composed of fibres, the shearing effect strongly influence the fibres structural properties, and the prevalent fibre shortening in turn leads to a decrease in the material's mechanical properties (Young's modulus 1.7 MPa, stress at break 0.2 MPa, elongation at break 9%). This effect is also observed in the reprocessed material (12 DAC-40gly_rep). While reprocessing doesn't strongly affect the thermal decomposition properties of the material, the shear stresses imposed on the fibres results in a change in fibres structure and shortening, which consecutively reflect in decreased mechanical properties (Young's modulus 2.7 MPa, stress at break 0.4 MPa, elongation at break 18%). Even if the melt viscosity during compounding doesn't reach the high values seen for 6.5 DAC-40gly, it must be remembered that the material has been processed twice, with shear stresses being applied to the fibres. In any case, the two processes that 12 DAC-40gly_rep has undergone still result in higher mechanical properties than 6.5 DAC-40gly, where the high shear stresses imposed during compounding have had a larger detrimental effect.

3.6. Cryo-fractured surfaces morphology assessed by scanning electron microscopy (SEM)

The investigation of the materials' morphologies was conducted through scanning electron microscopy on cryo-fractured surfaces, with the results presented in Fig. 6.

DAC melt processing without the addition of glycerol results in a smooth and uniform surface, typical of a brittle fracture (Fig. 6a). It is important to note that the inherent core-shell structure of DAC fibres cannot be observed due to the good interpenetration between the fibres upon solidification, which is a result of the higher mobility on the melt of the amorphous, thermoplastic shell. Nevertheless, at higher magnifications (1.0 kX), a textured surface becomes evident, which may be indicative of the presence of a fibre that was removed during the fracture. Additionally, at higher magnifications the surface displays the emergence of fibre heads (1.0 kX), thereby corroborating the fibrous nature of the material. The addition of glycerol to the system resulted in the observation of some pores on the surface (Fig. 6a). At higher magnifications (1.0 kX), the presence of fibres and their morphology was clearly discernible within some of the observed pores. The striation observed on the fibre surface is recognisable in areas of the surfaces where fibres have been extracted, as previously observed in 60 DAC. To elucidate the mechanical behaviour observed in the tensile test, a potential explanation for the reduction in elongation at break following the addition of an excess of glycerol could be provided by considering the possibility of a glycerol phase separation [51,64]. However, higher porosity with an excess of glycerol (60 DAC-40gly compared to 60 DAC-18gly) would have been expected, which is not visible. The registered decrease in elongation at break can be also ascribed to a phase inversion due to the different viscosities of phase separated DAC and glycerol at the processing temperature, which leads to a too soft and unstable material [64].

A comparison of the surfaces of the materials melt-compounded with the same glycerol content was investigated (Fig. 6b). The reprocessed material (12 DAC-40gly_rep) exhibits a higher porosity in comparison to 60 DAC-40gly. This phenomenon may be attributed to the migration of glycerol during the second melt compounding. These findings elucidate the subsequent decline in mechanical properties. Furthermore, the material melt compounded without any added water (6.5 DAC-40gly) also exhibits a slight increase in porosity in comparison to 60 DAC-40gly. The

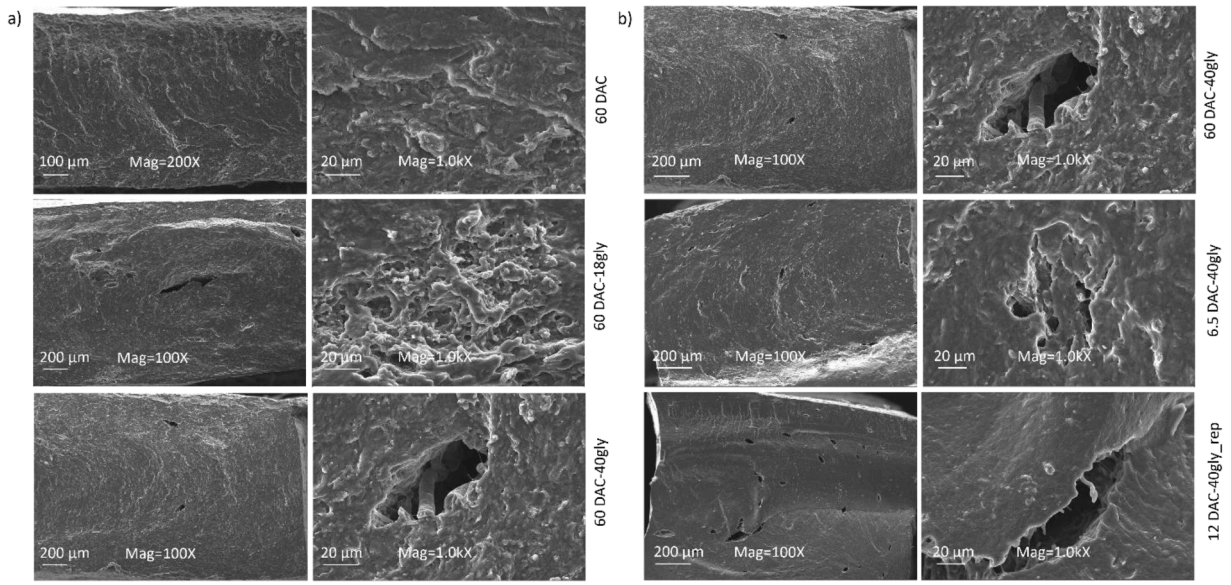


Fig. 6. Scanning electron microscopies on cryo-fractured surfaces of materials melt compounded with different glycerol contents (0, 18, 40 phr) (a) and moisture contents (60, 12 and 6.5 phr) (b). Different magnifications have been chosen for the surface morphological analysis (100, 200X and 1.0 kX).

elevated shear stresses imposed on the fibres due to the high viscosities observed during processing, coupled with the lower absorption of glycerol by DAC in comparison to the absorption of a water-glycerol solution, would lead to the incipient glycerol phase separation, ultimately resulting in a reduction in mechanical properties.

4. Conclusions

This study explored the possibility of replacing water with glycerol, as an alternative hydrophilic green plasticizer for stable primary and secondary shaping of thermoplastic dialcohol cellulose (DAC) fibres. The aim is to obtain materials whose properties are less affected by the moisture content (that depends on the environmental conditions, *e.g.* temperature, relative humidity) than water plasticized DAC fibres. A degree of modification of 46% from cellulose fibres to DAC was chosen for the study, and moisture and glycerol contents varied, for highlighting the neat effect of water *vs*. glycerol interaction with DAC fibres during and after the compounding and injection moulding at constant processing parameters.

From the in-line melt viscosity during compounding, the addition of increasing glycerol has an impact on reducing the melt viscosities, improving the material's melt processability. Once the glycerol addition exceeds a certain threshold (above 18 phr), the reduction in melt viscosity is no longer evident, pointing at a saturation threshold for the use of glycerol as an effective plasticizer. By thermogravimetric analysis, can be observed that even if the DAC onset temperature is reduced by the addition of glycerol, this has the effect of enhancing the thermal stability of the DAC amorphous phase (from 274 °C for 60 DAC to a maximum of 286 °C for 60 DAC-18gly), indicating DAC-glycerol strong interactions. These interactions are also confirmed by FTIR spectra, through increased water absorption following the addition of the hygroscopic glycerol to the system.

The glass-rubber transition temperatures, evaluated by MDSC and DMTA, decrease by increasing the glycerol content, demonstrating glycerol plasticizing effect, which after a certain amount intercalates between DAC fibres depleting fibre-fibre mutual interactions. The plasticization is also observed from the changed thermo-mechanical and tensile properties, evaluated from DMTA and tensile test. The increasing glycerol content results in a decrease in the material's elasticity (decrease of storage and Young's moduli), stress at break, and in an increase in the elongation at break. Nevertheless, the enhancement in deformability is not linear with the glycerol addition. The results showed that exceeding a certain threshold of added glycerol (above 18 phr) led to a reduction in the overall mechanical properties. The morphological analysis of cryo-fractured surfaces of glycerol plasticized DAC after the glycerol saturation threshold (>18 phr) was not conclusive for explain the registered drop in the mechanical properties due to glycerol phase separation. A possible formation of inter-fibre glycerol layer, hindering fibre-fibre mutual interactions, and/or a phase inversion could also explain the decrease of mechanical performance of oversaturated glycerol plasticized DAC fibre systems.

For comparison, DAC fibres were melt-processed by using only the DAC fibre moisture at the equilibrium (6.5 DAC-40gly), without the addition of fresh water. This resulted in drastically higher melt viscosities, necessitating significant quantities of glycerol (40 phr) to enable the melt processing. High viscosities, *i.e.* high shear stresses imposed on the material during compounding, result in reduced mechanical properties.

Furthermore, the feasibility of post-industrial mechanical recycling of the DAC fibres processed with the higher moisture and glycerol contents (12 DAC-40gly_rep) has been demonstrated. The reprocessing leads to a reduction in the material's final mechanical properties, without a significantly impact on its thermal stability. The decrease in the mechanical performance can be ascribed to the additional shear stresses in temperature to which the system is subjected during the recycling, which presumably influences the fibre structure, *i.e.* shortening.

In conclusion, to guarantee a reliable thermoplastic material that possesses high thermal stability, and increased deformability at the expenses of a moderate reduction in elasticity, the addition of glycerol up to a saturation point (about 18phr) should be considered. Water should be added to assist the DAC melt compounding, allowing the addition of lower glycerol contents and limiting the shear stresses imposed on the material, therefore preventing a detrimental effect on the final mechanical performance.

CRediT authorship contribution statement

Enrica Pellegrino: Writing – original draft, Visualization, Validation, Investigation, Formal analysis, Data curation. **Katarina Jonasson:** Writing – review & editing, Validation, Supervision, Investigation. **Alberto Fina:** Writing – review & editing, Validation, Supervision,

Resources. **Giada Lo Re:** Writing – review & editing, Validation, Supervision, Software, Resources, Project administration, Methodology, Funding acquisition, Formal analysis, Conceptualization.

Declaration of competing interest

The authors declare that they have no known competing financial interests or personal relationships that could have appeared to influence the work reported in this paper.

Acknowledgement

The authors acknowledge VINNOVA through the project Bio-Innovation ProDAC (grant number 2021-02094) for financial support. The authors acknowledge SCA Forest Products and FibRe (grant number 2019-00047) for in-kind support.

Data availability

Data will be made available on request.

References

[1] Cumulative Plastic Production Volume Worldwide from 1950 to 2050, 2024. https://www.statista.com/statistics/1019758/plastics-production-volume-worldwide/. Accessed: September.
[2] I. Mutmainna, P.L. Gareso, S. Suryani, D. Tahir, Microplastics from petroleum-based plastics and their effects: a systematic literature review and science mapping of global bioplastics production, Integr. Environ. Assess Manag. 20 (6) (2024) 1892–1911, https://doi.org/10.1002/ieam.4976.
[3] W.W.Y. Lau, et al., Evaluating scenarios toward zero plastic pollution, Science 369 (6510) (2020) 1455–1461, https://doi.org/10.1126/SCIENCE.ABA9475.
[4] C. Li, J. Wu, H. Shi, Z. Xia, J. Sahoo, J. Yeo, D.L. Kaplan, Fiber-based biopolymer processing as a route toward sustainability, Adv. Mater. 34 (1) (2022) 2105196, https://doi.org/10.1002/adma.202105196.
[5] Bioplastics Market Development Update 2023, 2024. https://www.european-bioplastics.org/market/. Accessed: September.
[6] C. Nawrath, Y. Poirier, C. Somerville, Plant polymers for biodegradable plastics: cellulose, starch and polyhydroxyalkanoates, Molecular Breed. 1 (1995) 105–122, https://doi.org/10.1007/BF01249696, 1995.
[7] G. Henriksson, H. Lennholm, Cellulose and carbohydrate chemistry, Wood Chem. Wood Biotechnol. (2009) 71–100.
[8] Y. Li, et al., The major role of London dispersion interaction in the assembly of cellulose, chitin, and chitosan, Cellulose 30 (13) (2023) 8127–8138, https://doi.org/10.1007/s10570-023-05376-5.
[9] M. Wohlert, T. Benselfelt, L. Wågberg, I. Furó, L.A. Berglund, J. Wohlert, Cellulose and the role of hydrogen bonds: not in charge of everything, Cellulose 2022 (2022) 1–23, https://doi.org/10.1007/s10570-021-04325-4.
[10] P. Cazón, G. Velazquez, J.A. Ramírez, M. Vázquez, Polysaccharide-based films and coatings for food packaging: a review, Food Hydrocoll. 68 (2017) 136–148, https://doi.org/10.1016/j.foodhyd.2016.09.009.
[11] E. Pellegrino, B. Al-Rudainy, P.A. Larsson, A. Fina, G. Lo Re, Impact of water plasticization on dialcohol cellulose fibres melt processing-structure-properties relationship, Carbohydrate Polymer Technol. Appl. 9 (2025) 100642.
[12] A. Lejeune, T. Deprez, Cellulose: Structure and properties, Derivatives and Industrial Uses, 2010, Nova Science Publishers, Incorporated, 2010.
[13] K. Müller, C. Zollfrank, M. Schmid, Natural polymers from biomass resources as feedstocks for thermoplastic materials, Macromol. Mater Eng. 304 (5) (2019) 1800760, https://doi.org/10.1002/mame.201800760, 2019.
[14] K. Immonen, et al., Thermoplastic cellulose-based compound for additive manufacturing, Molecules 26 (6) (2021) 1701, https://doi.org/10.3390/molecules26061701.
[15] S.H. Zeronian, F.L. Hudson, R.H. Peters, The mechanical properties of paper made from periodate oxycellulose pulp and from the same pulp after reduction with borohydride, Tappi 47 (1964) 557–564.
[16] W. Kasai, T. Morooka, M. Ek, Mechanical properties of films made from dialcohol cellulose prepared by homogeneous periodate oxidation, Cellulose 21 (1) (2014) 769–776, https://doi.org/10.1007/s10570-013-0153-7.
[17] P.A. Larsson, L.A. Berglund, L. Wågberg, Highly ductile fibres and sheets by core-shell structuring of the cellulose nanofibrils, Cellulose 21 (1) (2014) 323–333, https://doi.org/10.1007/s10570-013-0099-9.
[18] N. Guigo, K. Mazeau, J.L. Putaux, L. Heux, Surface modification of cellulose microfibrils by periodate oxidation and subsequent reductive amination with benzylamine: a topochemical study, Cellulose 21 (6) (2014) 4119–4133, https://doi.org/10.1007/s10570-014-0459-0.
[19] J.J. Benitez, et al., Transparent, plasticized cellulose-glycerol bioplastics for food packaging applications, Int. J. Biol. Macromol. 273 (2024) 132956, https://doi.org/10.1016/j.ijbiomac.2024.132956.
[20] G. Lo Re, et al., Melt processable cellulose fibres engineered for replacing oil-based thermoplastics, Chem. Eng. J. 458 (2023) 141372, https://doi.org/10.1016/j.cej.2023.141372.
[21] A.Y. Mehandzhiyski, E. Engel, P.A. Larsson, G. Lo Re, I.V. Zozoulenko, Microscopic insight into the structure–processing–property relationships of core–shell structured dialcohol cellulose nanoparticles, ACS Appl. Bio Mater. 5 (10) (2022) 4793–4802, https://doi.org/10.1021/acsabm.2c00505.
[22] E. Engel, G. Lo Re, P.A. Larsson, Melt processing of chemically modified cellulosic fibres with only water as plasticiser: effects of moisture content and processing temperature, Carbohydr. Polym. 348 (2025) 122891.
[23] H.D. Özeren, X.F. Wei, F. Nilsson, R.T. Olsson, M.S. Hedenqvist, Role of hydrogen bonding in wheat gluten protein systems plasticized with glycerol and water, Polymer 232 (2021) 124149, https://doi.org/10.1016/j.polymer.2021.124149.
[24] M.G.A. Vieira, M.A. Da Silva, L.O. Dos Santos, M.M. Beppu, Natural-based plasticizers and biopolymer films: a review, Eur. Polym J. 47 (3) (2011) 254–263, https://doi.org/10.1016/j.eurpolymj.2010.12.011.
[25] S. Agarwal, Major factors affecting the characteristics of starch based biopolymer films, Eur. Polym J. 160 (2021) 110788, https://doi.org/10.1016/j.eurpolymj.2021.110788.
[26] R. Thakur, P. Pristijono, C.J. Scarlett, M. Bowyer, S.P. Singh, Q.V. Vuong, Starch-based films: major factors affecting their properties, Int. J. Biol. Macromol. 132 (2019) 1079–1089, https://doi.org/10.1016/j.ijbiomac.2019.03.190.
[27] Z.Y. Ben, H. Samsudin, M.F. Yhaya, Glycerol: its properties, polymer synthesis, and applications in starch based films, Eur. Polym J. 175 (2022) 111377, https://doi.org/10.1016/j.eurpolymj.2022.111377.
[28] C.E. Montilla-Buitrago, R.A. Gómez-López, J.F. Solanilla-Duque, L. Serna-Cock, H. S. Villada-Castillo, Effect of plasticizers on properties, retrogradation, and processing of extrusion-obtained thermoplastic starch: a review, Starch-Stärke 73 (9–10) (2021) 2100060, https://doi.org/10.1002/star.202100060.
[29] M. Bocqué, C. Voirin, V. Lapinte, S. Caillol, J.J. Robin, Petro-based and bio-based plasticizers: chemical structures to plasticizing properties, J. Polymer Sci. Part A: Polymer Chem. 54 (1) (2016) 11–33, https://doi.org/10.1002/pola.27917.
[30] V. Epure, M. Griffon, E. Pollet, L. Avérous, Structure and properties of glycerol-plasticized chitosan obtained by mechanical kneading, Carbohydr. Polym. 83 (2) (2011) 947–952, https://doi.org/10.1016/j.carbpol.2010.09.003.
[31] S. Keshanidokht, S. Kumar, P.W. Thulstrup, M.A. Via, M.P. Clausen, J. Risbo, Thermo-responsive behavior of glycerol-plasticized oleogels stabilized by zein, Food Hydrocoll. 139 (2023) 108582, https://doi.org/10.1016/j.foodhyd.2023.108582.
[32] J.J.G. Van Soest, N. Knooren, Influence of glycerol and water content on the structure and properties of extruded starch plastic sheets during aging, J. Appl. Polym Sci. 64 (7) (1997) 1411–1422, https://doi.org/10.1002/(SICI)1097-4628(19970516)64:7<1411::AID-APP21>3.0.CO;2-Y.
[33] E. Basiak, A. Lenart, F. Debeaufort, How glycerol and water contents affect the structural and functional properties of starch-based edible films, Polymers 10 (4) (2018) 412, https://doi.org/10.3390/polym10040412.
[34] P.A. Larsson, L. Wågberg, Towards natural-fibre-based thermoplastic films produced by conventional papermaking, Green Chem. 18 (11) (2016) 3324–3333, https://doi.org/10.1039/c5gc03068d.
[35] H. Zhao, N.D. Heindel, Determination of degree of substitution of formyl groups in polyaldehyde dextran by the hydroxylamine hydrochloride method, Pharm. Res. 8 (1991) 400–402, https://doi.org/10.1023/A:1015866104055.
[36] D. Lourdin, L. Coignard, H. Bizot, P. Colonna, Influence of equilibrium relative humidity and plasticizer concentration on the water content and glass transition of starch materials, Polymer 38 (21) (1997) 5401–5406, https://doi.org/10.1016/S0032-3861(97)00082-7.
[37] J. Tarique, S.M. Sapuan, A. Khalina, Effect of glycerol plasticizer loading on the physical, mechanical, thermal, and barrier properties of arrowroot (Maranta arundinacea) starch biopolymers, Sci. Rep. 11 (1) (2021) 13900, https://doi.org/10.1038/s41598-021-93094-y.
[38] N. Khotsaeng, W. Simchuer, T. Imsombut, P. Srihanam, Effect of glycerol concentrations on the characteristics of cellulose films from cattail (Typha angustifolia L.) Flowers, Polymers 15 (23) (2023) 4535, https://doi.org/10.3390/polym15234535.
[39] W. Gao, et al., Development and characterization of starch films prepared by extrusion blowing: the synergistic plasticizing effect of water and glycerol, Lwt 148 (2021) 111820, https://doi.org/10.1016/j.lwt.2021.111820.
[40] B. Janković, Thermal characterization and detailed kinetic analysis of Cassava starch thermo-oxidative degradation, Carbohydr. Polym. 95 (2) (2013) 621–629, https://doi.org/10.1016/j.carbpol.2013.03.038.
[41] G. Ayala, A. Agudelo, R. Vargas, Effect of glycerol on the electrical properties and phase behavior of cassava starch biopolymers, Dyna 79 (171) (2012) 138–147.
[42] P.R. Chang, R. Jian, P. Zheng, J. Yu, X. Ma, Preparation and properties of glycerol plasticized-starch (GPS)/cellulose nanoparticle (CN) composites, Carbohydr. Polym. 79 (2) (2010) 301–305, https://doi.org/10.1016/j.carbpol.2009.08.007.
[43] V. Hospodarova, E. Singovszka, N. Stevulova, Characterization of cellulosic fibers by FTIR spectroscopy for their further implementation to building materials, Am. J. Anal. Chem. 9 (6) (2018) 303–310, https://doi.org/10.4236/ajac.2018.96023.
[44] A. Célino, O. Gonçalves, F. Jacquemin, S. Fréour, Qualitative and quantitative assessment of water sorption in natural fibres using ATR-FTIR spectroscopy, Carbohydr. Polym. 101 (2014) 163–170, https://doi.org/10.1016/j.carbpol.2013.09.023.
[45] F. Carrillo, X. Colom, J.J. Suñol, J. Saurina, Structural FTIR analysis and thermal characterisation of lyocell and viscose-type fibres, Eur. Polym. J. 40 (9) (2004) 2229–2234, https://doi.org/10.1016/j.eurpolymj.2004.05.003.

[46] P. Cazón, M. Vázquez, G. Velazquez, Cellulose-glycerol-polyvinyl alcohol composite films for food packaging: evaluation of water adsorption, mechanical properties, light-barrier properties and transparency, Carbohydr. Polym. 195 (2018) 432–443, https://doi.org/10.1016/j.carbpol.2018.04.120.
[47] S. Van Nguyen, B.K. Lee, Microfibrillated cellulose film with enhanced mechanical and water-resistant properties by glycerol and hot-pressing treatment, Cellulose 28 (9) (2021) 5693–5705, https://doi.org/10.1007/s10570-021-03894-8.
[48] D. Muscat, B. Adhikari, R. Adhikari, D.S. Chaudhary, Comparative study of film forming behaviour of low and high amylose starches using glycerol and xylitol as plasticizers, J. Food Eng. 109 (2) (2012) 189–201, https://doi.org/10.1016/j.jfoodeng.2011.10.019.
[49] S.M. Gonçalves, D.C. dos Santos, J.F.G. Motta, R.R. dos Santos, D.W.H. Chávez, N. R. de Melo, Structure and functional properties of cellulose acetate films incorporated with glycerol, Carbohydr. Polym. 209 (2019) 190–197, https://doi.org/10.1016/j.carbpol.2019.01.031.
[50] E.A. Arik Kibar, F. Us, Thermal, mechanical and water adsorption properties of corn starch-carboxymethylcellulose/methylcellulose biodegradable films, J. Food Eng. 114 (1) (2013) 123–131, https://doi.org/10.1016/j.jfoodeng.2012.07.034.
[51] M. Sanyang, S. Sapuan, M. Jawaid, M. Ishak, J. Sahari, Effect of plasticizer type and concentration on tensile, thermal and barrier properties of biodegradable films based on sugar palm (Arenga pinnata) starch, Polymers 7 (6) (2015) 1106–1124, https://doi.org/10.3390/polym7061106.
[52] D. Lourdin, L. Coignard, H. Bizot, P. Colonna, Influence of equilibrium relative humidity and plasticizer concentration on the water content and glass transition of starch materials, Polymer 38 (21) (1997) 5401–5406.
[53] R. Shi, et al., Ageing of soft thermoplastic starch with high glycerol content, J. Appl. Polym. Sci. 103 (1) (2007) 574–586, https://doi.org/10.1002/app.25193.
[54] N.L. García, L. Ribba, A. Dufresne, M. Aranguren, S. Goyanes, Effect of glycerol on the morphology of nanocomposites made from thermoplastic starch and starch nanocrystals, Carbohydr. Polym. 84 (1) (2011) 203–210, https://doi.org/10.1016/j.carbpol.2010.11.024.
[55] G. Östberg, L. Salmén, J. Terlecki, Softening temperature of moist wood measured by differential scanning calorimetry, Holzforschung (1990) 223–225, https://doi.org/10.1515/hfsg.1990.44.3.223.
[56] K.M. Picker, S.W. Hoag, Characterization of the thermal properties of microcrystalline cellulose by modulated temperature differential scanning calorimetry, J. Pharm. Sci. 91 (2) (2002) 342–349, https://doi.org/10.1002/jps.10018.
[57] L. Mościcki, M. Mitrus, A. Wójtowicz, T. Oniszczuk, A. Rejak, L. Janssen, Application of extrusion-cooking for processing of thermoplastic starch (TPS), Food Res. Int. 47 (2) (2012) 291–299, https://doi.org/10.1016/j.foodres.2011.07.017.
[58] M. Ghasemlou, F. Khodaiyan, A. Oromiehie, Physical, mechanical, barrier, and thermal properties of polyol-plasticized biodegradable edible film made from kefiran, Carbohydr. Polym. 84 (1) (2011) 477–483, https://doi.org/10.1016/j.carbpol.2010.12.010.
[59] M. Jouki, N. Khazaei, M. Ghasemlou, M. Hadinezhad, Effect of glycerol concentration on edible film production from cress seed carbohydrate gum, Carbohydr. Polym. 96 (1) (2013) 39–46, https://doi.org/10.1016/j.carbpol.2013.03.077.
[60] O.V. López, C.J. Lecot, N.E. Zaritzky, M.A. García, Biodegradable packages development from starch based heat sealable films, J. Food. Eng. 105 (2) (2011) 254–263, https://doi.org/10.1016/j.jfoodeng.2011.02.029.
[61] J. Sahari, S.M. Sapuan, E.S. Zainudin, M.A. Maleque, Thermo-mechanical behaviors of thermoplastic starch derived from sugar palm tree (Arenga pinnata), Carbohydr. Polym. 92 (2) (2013) 1711–1716, https://doi.org/10.1016/j.carbpol.2012.11.031.
[62] N. Laohakunjit, A. Noomhorm, Effect of plasticizers on mechanical and barrier properties of rice starch film, Starch-Stärke 56 (8) (2004) 348–356, https://doi.org/10.1002/star.200300249.
[63] A.C. Souza, R. Benze, E.S. Ferrão, C. Ditchfield, A.C.V. Coelho, C.C. Tadini, Cassava starch biodegradable films: influence of glycerol and clay nanoparticles content on tensile and barrier properties and glass transition temperature, LWT-Food Sci. Technol. 46 (1) (2012) 110–117, https://doi.org/10.1016/j.lwt.2011.10.018.
[64] F. Xie, et al., Characteristics of starch-based films plasticised by glycerol and by the ionic liquid 1-ethyl-3-methylimidazolium acetate: a comparative study, Carbohydr. Polym. 111 (2014) 841–848, https://doi.org/10.1016/j.carbpol.2014.05.058.
[65] E.D.R. Zavareze, et al., Development of oxidised and heat-moisture treated potato starch film, Food Chem. 132 (1) (2012) 344–350, https://doi.org/10.1016/j.foodchem.2011.10.090.